Governing Equations, Numerical Methods, Validation, and Interpretive Limits

Version 1.0 | Stella Nova Education and Research Center | 2026

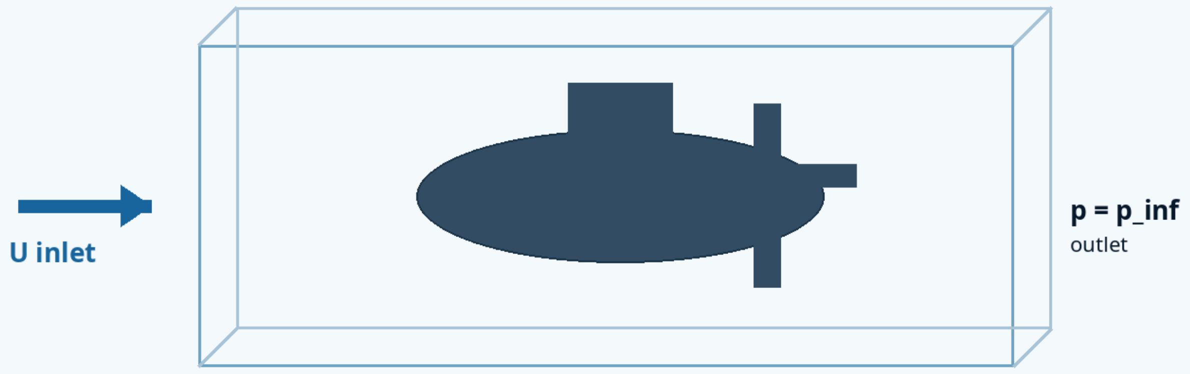

Virtual water tunnel domain

Purpose

The Hydrodynamic Flow Model Tester (HFMT) is a browser-based virtual water tunnel for fully submerged objects. It accepts preset geometries or local STL uploads, estimates hydrodynamic resistance in a fast analytical preview, and optionally runs a coarse three-dimensional lattice-Boltzmann flow solve. The interface is intended for design comparison, teaching, and preliminary research reasoning.

Interpretive limit

HFMT is not a substitute for a validated engineering CFD workflow, a towing-tank experiment, or a certification analysis. Numerical accuracy depends on model scale, mesh integrity, grid resolution, boundary clearance, Reynolds similarity, convergence, and the validity of the selected fluid assumptions.

Privacy

Uploaded STL geometry is parsed and rendered in the browser. It is not transmitted to the Stella Nova server. The no-database annotation system stores only user-entered scholarly comments in a server-local JSON file.

1. Scope and operating assumptions

- The modeled object is fully submerged. Free-surface wave resistance is excluded.
- The fluid is treated as incompressible and isothermal during each run.
- Version 1 models passive geometry and fixed appendages. Propellers, pumps, rotating parts, and fluid-structure interaction are excluded.
- Freshwater and seawater properties are calculated from user-selected temperature, salinity, and depth.
- The fast preview is an analytical and geometric estimate. The numerical mode is a coarse browser-resident flow solver.
- Cavitation is reported as a screening margin. Multiphase bubble dynamics are not solved.

The tool exposes the assumptions that materially affect interpretation. Each report records characteristic length, water properties, projected area, wetted area, blockage ratio, solver grid, iteration count, residual, and effective lattice Reynolds number.

STL scale handling

STL files normally contain triangulated coordinates but no reliable physical-unit metadata. The user must confirm units and known overall length. Surface area scales with the square of the length conversion, and enclosed volume scales with its cube. Open, self-intersecting, or non-manifold meshes can produce unreliable volume and voxelization results.

2. Fluid properties

Density and viscosity are not cosmetic controls. They determine Reynolds number, dynamic pressure, viscous resistance, hydrostatic pressure, and cavitation margin.

Kinematic viscosity

$$\nu = \frac{\mu}{\rho} \tag{1}$$

Here ρ is fluid density, μ is dynamic viscosity, and ν is kinematic viscosity.

Hydrostatic ambient pressure

$$p_\infty = p_{\text{surface}} + \rho g h \tag{2}$$

Depth h is converted to absolute ambient pressure using standard gravitational acceleration. For preliminary browser calculations, density is pressure-corrected using a bulk-modulus approximation.

Freshwater

Freshwater density is approximated over the normal liquid-water temperature range, while dynamic viscosity follows the temperature-sensitive ordinary-water relationship used by the interface. For authoritative water-property calculations, consult the current IAPWS releases.

Seawater

The interface uses a compact EOS-80-style density approximation for immediate interaction and records Absolute Salinity in g/kg. The methodology and future high-precision modules use TEOS-10 as the thermodynamic reference framework. TEOS-10 distinguishes Absolute Salinity from Practical Salinity and provides internally consistent thermodynamic properties of seawater.

Vapor pressure

Water vapor pressure is estimated from temperature and is used only in the cavitation-number screening calculation. Dissolved gas, nuclei population, surface defects, and transient pressure history are not represented.

3. Governing equations and dimensionless quantities

Continuity for incompressible flow

$$\nabla \cdot \mathbf{u} = 0 \tag{3}$$

Momentum equation

$$\frac{\partial \mathbf{u}}{\partial t} + (\mathbf{u} \cdot \nabla)\mathbf{u} = -\frac{1}{\rho}\nabla p + \nu \nabla^2 \mathbf{u} \tag{4}$$

This incompressible Navier-Stokes form expresses transient acceleration, convective acceleration, pressure-gradient acceleration, and viscous diffusion.

Reynolds number

$$Re = \frac{UL}{\nu} = \frac{\rho UL}{\mu} \tag{5}$$

U is the reference water speed and L is the confirmed characteristic length. Reynolds number is central to dynamic similarity. A coarse browser grid cannot reproduce the full range of engineering Reynolds numbers; the numerical solver therefore reports its effective lattice Reynolds number separately from the physical target Reynolds number.

Dynamic pressure

$$q = \frac{1}{2}\rho U^2 \tag{6}$$

Surface force

$$\mathbf{F} = \int_S (-p\mathbf{n} + \boldsymbol{\tau} \cdot \mathbf{n})\, dA \tag{7}$$

The pressure term contributes form or pressure resistance. The viscous stress term contributes skin-friction resistance.

Drag coefficient

$$C_D = \frac{F_D}{\frac{1}{2}\rho U^2 A_{\text{ref}}} \tag{8}$$

Pressure coefficient

$$C_p = \frac{p - p_\infty}{\frac{1}{2}\rho U^2} \tag{9}$$

4. Analytical preview

The analytical preview is designed to remain responsive while the user rotates the body, changes speed, or adjusts water conditions. It combines exact or mesh-derived geometry measures with empirical resistance relationships.

Geometry measures

- Wetted surface area is calculated by summing triangle areas after physical scaling.
- Enclosed volume is estimated from signed tetrahedral volumes and is reliable only for consistently oriented closed meshes.
- Projected frontal, top, and side areas are estimated from area-weighted surface-normal projections.
- Characteristic length is the confirmed overall model length.
- Blockage ratio compares maximum projected area with the selected virtual tunnel area.

Turbulent skin-friction reference

$$C_F = \frac{0.075}{(\log_{10} Re - 2)^2} \tag{10}$$

The ITTC-1957 line is used as a smooth turbulent friction reference. It does not represent total drag of an arbitrary body. HFMT applies a form-factor term and a separate pressure-drag estimate. Surface roughness adds a documented friction allowance.

Resistance power

$$P_D = F_D U \tag{11}$$

The preview surface coloring is interpretive. Pressure coloring is derived from surface orientation relative to the incoming flow and longitudinal position. Wall-shear coloring emphasizes tangential flow exposure. Separation and wake overlays are risk visualizations, not direct solutions of local turbulent structures.

5. Numerical flow solver

The numerical mode uses a three-dimensional, nineteen-velocity lattice-Boltzmann formulation (D3Q19) implemented in a browser Web Worker. The worker prevents the interface from freezing while geometry is voxelized and the flow field iterates.

Discrete evolution

$$f_i(\mathbf{x} + \mathbf{c}_i\Delta t, t + \Delta t) = f_i(\mathbf{x}, t) - \omega\left[f_i - f_i^{eq}\right] \tag{12}$$

The initial implementation uses a single-relaxation-time BGK collision operator for portability. The architecture separates the worker so that a multiple-relaxation-time operator can replace it without changing the visual interface or data contract.

Macroscopic recovery

$$\rho = \sum_i f_i \qquad \rho\mathbf{u} = \sum_i f_i\mathbf{c}_i \tag{13}$$

Relaxation and lattice viscosity

$$\nu_{LB} = \frac{\tau - \frac{1}{2}}{3} \tag{14}$$

Geometry voxelization

The uploaded triangle mesh is transformed to the selected yaw, pitch, and roll, scaled into the numerical domain, and converted into a solid-cell mask by ray intersections through the triangulated surface. The solver records the number of solid cells and open intersection columns. A fallback ellipsoidal mask is used only when a mesh cannot be closed numerically, and the geometry diagnostic should then be treated as a warning.

Boundary conditions

- Velocity inlet: equilibrium populations are prescribed at the upstream boundary.
- Pressure-like outlet: downstream populations are extrapolated from the adjacent interior plane.
- Object surface: no-slip bounce-back with momentum exchange.
- Open-water side boundaries: periodic far-field approximation.
- Bounded-tunnel side boundaries: bounce-back walls.

Reynolds similarity cap

Engineering-scale Reynolds numbers can exceed the stable range of a coarse weakly compressible lattice. HFMT therefore caps the lattice Reynolds number and reports the effective value. Numerical output is used primarily to refine relative wake and pressure-drag behavior, while the physical-unit resistance estimate remains anchored to the analytical model.

6. Visualization layers

The viewport is an interpretive instrument. Each layer can be toggled independently so the user can distinguish model geometry from calculated or inferred flow information.

Layer	Meaning	Status
Model	Triangulated uploaded or preset geometry	Direct geometry
Streamlines	Seeded paths displaced around the body envelope	Preview visualization
Particles	Animated tracers following the streamline family	Preview visualization
Velocity	Numerical center-plane speed field after a solve	Computed numerical slice
Pressure Cp	Orientation-based preview coloring; numerical refinement planned	Interpretive preview
Wall shear	Tangential-exposure indicator	Interpretive preview
Separation	Curvature, aft-body, and incidence risk	Interpretive preview
Wake	Animated downstream deficit and vortex proxy	Preview or solver-informed
Forces	Total drag, lift, and side-force vectors	Calculated output
Cavitation	Low-pressure screening relative to ambient and vapor pressure	Risk indicator

7. Cavitation screening and pressure interpretation

Cavitation number

$$\sigma = \frac{p_\infty - p_v}{\frac{1}{2}\rho U^2} \quad (15)$$

Lower cavitation number generally indicates reduced pressure margin. HFMT compares ambient absolute pressure with water vapor pressure at the selected temperature. A body can experience local pressures below the free-stream value, so a surface pressure-coefficient estimate is also needed when screening specific locations.

Not included

- Nucleation-site distributions and dissolved-gas effects
- Sheet, cloud, tip-vortex, or bubble cavitation dynamics
- Two-phase compressibility and collapse pressure
- Material erosion, acoustic emission, or propulsor cavitation

The cavitation overlay must therefore be read as a design-warning layer, not as a prediction of bubble extent or damage.

8. Validation and benchmark pathway

Validation is staged. A browser visualizer should not claim engineering credibility merely because it displays a converged residual.

- Canonical geometry checks: sphere, cube, cylinder, prolate spheroid, flat plate, and NACA 0012 hydrofoil.
- Geometry checks: known analytical areas and volumes, scale conversion, and rotational invariance.
- Flow checks: Poiseuille flow and low-Re flow around simple obstacles for solver regression.
- Submarine benchmark: DARPA SUBOFF bare-hull and appended configurations using published geometry and experimental comparisons.
- Grid study: at least three resolutions with drag, wake deficit, and residual comparisons.
- Boundary study: tunnel-size and open-water comparisons to identify blockage sensitivity.
- Cross-solver study: export a geometry and condition package for comparison with OpenFOAM or another validated CFD package.

DARPA SUBOFF

The SUBOFF program produced an axisymmetric submarine benchmark with documented geometry and experimental data. HFMT's initial preset is inspired by this benchmark for interface testing. A research-grade validation release should use the published offsets and explicitly distinguish bare-hull, fairwater, and appended configurations.

9. Uncertainty, convergence, and reporting

A numerical residual is not a complete uncertainty estimate. The report should be interpreted through several independent checks.

Diagnostic	Why it matters	Recommended response
Mesh integrity	Open or self-intersecting STL can corrupt volume and voxelization	Repair geometry and repeat
Cells across diameter	Under-resolved curvature increases force error	Increase grid resolution
Blockage ratio	Narrow domains can inflate resistance	Increase tunnel dimensions
Residual history	Unsteady or diverging fields are not converged	Run longer or reduce lattice Re
Grid dependence	One resolution cannot establish numerical independence	Compare low, medium, and high
Reynolds mismatch	Lattice and physical flows may not be dynamically similar	Treat solver as qualitative and retain analytical scaling
Surface roughness	Skin friction can dominate streamlined bodies	Document coating or fouling assumption

The A/B laboratory is particularly valuable because relative comparisons under identical numerical settings are often more robust than isolated absolute predictions. Equal-length, equal-volume, or equal-frontal-area normalization must be stated in the comparison report.

10. References

1. Bouzidi, M., M. Firdaouss, and P. Lallemand. 2001. Momentum transfer of a Boltzmann-lattice fluid with boundaries. Physics of Fluids 13(11):3452-3459. https://doi.org/10.1063/1.1399290.

2. d'Humieres, D., I. Ginzburg, M. Krafczyk, P. Lallemand, and L.-S. Luo. 2002. Multiple-relaxation-time lattice Boltzmann models in three dimensions. Philosophical Transactions of the Royal Society A 360:437-451. https://doi.org/10.1098/rsta.2001.0955.

3. Groves, N. C., T. T. Huang, and M. S. Chang. 1989. Geometric Characteristics of DARPA SUBOFF Models. David Taylor Research Center Report DTRC/SHD-1298-01.

4. International Association for the Properties of Water and Steam (IAPWS). 2008. Release on the IAPWS Formulation 2008 for the Viscosity of Ordinary Water Substance. IAPWS R12-08.

5. International Towing Tank Conference (ITTC). 2024. Resistance Test. Recommended Procedures and Guidelines 7.5-02-02-01.

6. IOC, SCOR, and IAPSO. 2010. The International Thermodynamic Equation of Seawater - 2010: Calculation and Use of Thermodynamic Properties. Intergovernmental Oceanographic Commission, Manuals and Guides No. 56, UNESCO.

7. Lallemand, P., and L.-S. Luo. 2000. Theory of the lattice Boltzmann method: Dispersion, dissipation, isotropy, Galilean invariance, and stability. Physical Review E 61:6546-6562. https://doi.org/10.1103/PhysRevE.61.6546.

8. Qian, Y. H., D. d'Humieres, and P. Lallemand. 1992. Lattice BGK models for Navier-Stokes equation. Europhysics Letters 17(6):479-484. https://doi.org/10.1209/0295-5075/17/6/001.

9. White, F. M. 2011. Fluid Mechanics. 7th edition. McGraw-Hill, New York.

10. Zou, Q., and X. He. 1997. On pressure and velocity boundary conditions for the lattice Boltzmann BGK model. Physics of Fluids 9:1591-1598. https://doi.org/10.1063/1.869307.

Suggested citation

Stella Nova Education and Research Center. 2026. Hydrodynamic Flow Model Tester: Governing Equations, Numerical Methods, Validation, and Interpretive Limits. Version 1.0. Stella Nova Education and Research Center.